TOXICOLOGICAL SCIENCES **90(1)**, 87–95 (2006)
doi:10.1093/toxsci/kfj069
Advance Access publication December 9, 2005

Effect of PCB 126 on Hepatic Metabolism of Thyroxine and Perturbations in the Hypothalamic-Pituitary-Thyroid Axis in the Rat

Jeffrey W. Fisher,*[,1] Jerry Campbell,* Srinivasa Muralidhara,* James V. Bruckner,* Duncan Ferguson,* Moiz Mumtaz,† Barry Harmon,‡ Joan M. Hedge,§ Kevin M. Crofton,[¶] Hekap Kim,‖ and Tara L. Almekinder*

*University of Georgia, Interdisciplinary Toxicology Program, Athens, Georgia 30602; †Agency for Toxic Substances and Disease Registry (ATSDR), NCEH/ATSDR/DT, Chamblee, GA 30341; ‡University of Georgia, College of Veterinary Medicine, Department of Pathology, Athens, GA 30602; §USEPA/ORD/NHEERL, Neurotoxicology Division, Research Triangle Park, NC 27711; [¶]U.S. Environmental Protection Agency (USEPA/ORD/NHEERL) Neurotoxicology Division; and ‖Visiting Scientist, Department of Environmental Science, College of Natural Sciences, Kangwon, National University, Churcheon, Gangwon Do 200-701 South Korea

Received August 27, 2005; accepted November 23, 2005

The objective of this research was to examine the time- and dose- dependent disturbances in the hypothalamic-pituitary-thyroid (HPT) axis of adult male rats administered a potent coplanar (non-*ortho*) PCB, 3,3′,4,4′,5-pentachlorobiphenyl (PCB 126). Adult male Sprague-Dawley rats were administered a single oral bolus dose of 0, 7.5, 75, or 275 μg PCB 126/kg bw dissolved in corn oil. The rats were sacrificed periodically over 22 days. The 7.5-μg/kg dose induced hepatic ethoxyresorufin-O-deethylation EROD activity, but no changes were observed in hepatic uridine diphosphate glucuronyl transferases (UDPGTs) activity or serum TSH, T_4, or fT_4 concentrations. The two highest doses caused a modest decline in weight gain, induced hepatic EROD and UDPGT activities, increased serum TSH concentrations, and decreased serum T_4 and fT_4 concentrations. The amount of thyroxine glucuronide formed daily (pM/mg protein) increased linearly with the area-under-the-concentration-curve (AUCC) for PCB 126 in liver (μg/kg/day) and then slowed at the 275-μg/kg PCB 126 dose. Perturbations in the HPT axis were nonlinear with respect to PCB 126 dosing. As expected, an inverse relationship between the AUCC for serum T_4 (μg/dl/day) and the AUCC for serum TSH (ng/dl/day) was observed; however, the relationship was highly nonlinear. These data support a mode of action for PCB 126 involving induction of hepatic UDPGTs by the aryl hydrocarbon receptor AhR. However, the dose-response characteristics of the HPT axis are nonlinear and complex, requiring sophisticated tools, such as PBPK models, to characterize dose response.

Key Words: **PCB 126; thyroid hormones; P450, EROD; rat; TSH; UDPGT.**

Polychlorinated biphenyls (PCBs) were produced industrially from the years 1929 to 1977 for their unique chemical properties such as thermal stability, resistance to acids and bases, and low water solubility (ATSDR, 2000). Production was halted due to increasing awareness of health effects associated with PCB exposure. PCBs are very lipophilic and persistent in the environment. PCB congeners or mixtures (Aroclors) have been associated with various toxic responses including cancers, hepatotoxicity, gastrointestinal and respiratory disturbances, neurotoxicity, immunotoxicity, reproductive and developmental effects, and endocrine disruption including thyroid toxicity (ATSDR, 2000; Li and Hansen, 1997).

Thyroid hormones are critical for normal body metabolism, growth, development, and reproduction, and numerous toxicology studies with PCBs have documented the disruption of normal thyroid function in laboratory animals (Brouwer *et al.*, 1998). Dioxins and coplanar PCBs disrupt the hypothalamic-pituitary-thyroid (HPT) axis in laboratory animals (Beetstra *et al.*, 1991; Craft *et al.*, 2002; Desaulniers *et al.*, 1999; Martin, 2002; Van Birgelen *et al.*, 1994a,b) by binding to the aryl hydrocarbon receptor (AhR) and increasing transcription of several hepatic proteins including uridine diphosphate glucuronyl transferases (UDPGTs) (Auyeung *et al.*, 2003; Craft *et al.*, 2002; Schuur *et al.*, 1997). The induction of UDPGTs leads to increased glucuronidation of thyroxine (T_4) and subsequent excretion in bile as T_4-glucuronide (T_4-G). The increased loss of T_4 in bile and ultimately in feces is thought to result in disruption of the HPT axis (Hood and Klaassen, 2000). Nonplanar, *ortho* substituted PCB congeners do not bind to the AhR receptor, but do cause disturbances in the HPT axis, as evidenced by a decline in serum T_4 concentrations (e.g., Craft *et al.*, 2002; Desaulniers *et al.*, 1999; Van Birgelen *et al.*, 1994b). The decline in serum T_4 concentrations results from increased metabolism of thyroxine to T_4-G via upregulation of UDPGTs, but the induction of UDPGTs is controlled by the constitutive androstane receptor (CAR) and pregnane X receptors (PXR) (Kretschmer and Baldwin, 2005; Schuetz *et al.*, 1998). Other mechanisms for disruption of the HPT axis have been proposed for PCBs, including direct effects on TSH release in the pituitary (Khan *et al.*, 2003) and hydroxylated metabolites of PCBs displacing T_4 from serum binding proteins

[1] To whom correspondence should be addressed at University of Georgia, 206 Environmental Health Sciences Department, Athens, GA 30602–2102. Fax: (706) 542-7472. E-mail: jwfisher@uga.edu.

(transthyretin), potentially resulting in the accelerated systemic clearance of T_4 (Chauhan *et al.*, 2000; Cheek *et al.*, 1999; Lans *et al.*, 1993).

The ultimate objective of our research is to develop physiological models that describe the HPT axis in the rat to predict dose-dependent perturbations in the HPT axis by chemicals. In this paper we present a portion of the experimental findings for adult male rats administered a potent coplanar (non-*ortho*) PCB, 3,3′,4,4′,5-pentachlorobiphenyl (PCB 126). PCB 126 has been studied in the rat. In a 30-day rat kinetic study with PCB 126, Yoshimura *et al*. (1985) estimated that 70% of the PCB 126 dose was still present in the liver 5 days after dosing, and the serum PCB 126 half-life was approximately 17 days. The sequestration of PCB 126 in the liver represents substantial binding of PCB 126 to P450 cytochrome (CYP) 1A2 (Chen *et al.*, 2003). A primary concern of PCB 126 toxicity is its ''dioxin-like'' characteristics to cause cancer via the AhR receptor–mediated signaling pathways (Toyoshiba *et al.*, 2004). The National Toxicology Program has conducted a 2-year cancer bioassay on PCB 126 (NTP, 2005), including an evaluation of the thyroid.

Several acute research studies have examined the effects of PCB 126 on the HPT axis. PCB 126 causes consistent dose-related declines in serum T_4 concentrations and increases in hepatic CYP 1A1 and UDPGT activities (Craft *et al.*, 2002; Desaulniers *et al.*, 1999; Martin, 2002) with daily repeated doses of 2 to 7 days and dose rates ranging from 0.03 to 400 μg/kg/day. Serum T_3 concentrations were either unchanged (Martin, 2002) by PCB 126 administration or decreased (Desaulniers *et al.*, 1999). No consistent changes in TSH serum concentrations were found (Craft *et al.*, 2002; Desaulniers *et al.*, 1999).

There is a no time-course data published on the pharmacokinetics of PCB 126 in the rat, and there is no data published on the time- and dose-dependent changes of the HPT axis caused by PCB 126 in the rat. In the present study male adult rats were administered a single dose of 7.5, 75, or 275 μg/kg of PCB 126 by oral bolus intubation, and biological samples collected at various times after dosing. The goal was to collect temporal information on the kinetics of PCB 126 in the liver, the upregulation of hepatic enzymes, specifically UDPGT, which is responsible for the disruption of the HPT axis, and several biological indicators of thyroid status.

MATERIALS AND METHODS

Study design. Rats ($n = 104$) were administered a single oral bolus of PCB 126 in corn oil (0.0, 7.5, 75, or 275 μg/kg). The dosing volume was adjusted to give 1.0 ml/kg body weight. Eight rats were killed prior to dosing to obtain control information, and then eight rats per dose group (32 rats per sacrifice day) were killed on Days 5, 9, and 22. To embellish the PCB 126 pharmacokinetic studies, an additional 48 rats were dosed ($n = 4$ per dose group, excluding the control group) to obtain PCB 126 tissue concentrations of Days 1, 3, and 15 post dosing. Hepatic enzymes were measured on Day 1 in these rats.

Chemicals and reagents. PCB 126 was obtained from Accustandard Corporation (New Haven, CT) at purity greater than 99%. Stock solutions were prepared by dissolving PCB 126 in *n*-hexane, and the concentrations were checked by gas chromatography using a micro-electron capture detector (GC/μECD). The *n*-hexane and PCB 126 stock solutions were then mixed with corn oil (Mazola™, Best Foods, Englewood Cliffs, NJ), and then the *n*-hexane was removed by evaporation under a mild stream of nitrogen gas (adapted from DeVito *et al*., 1993). All solutions were prepared by dilution of equal amounts of hexane or hexane/PCB 126 with corn oil. Four dosing solutions were prepared (0.0, 7.5, 75, 275 μg/kg) with final concentrations of 0.0, 0.002, 0.020, and 0.0599 mg/ml, respectively.

Animals. Male Sprague-Dawley rats were obtained from Charles River Laboratories (Wilmington, MA) weighing 151–175 grams. Rats were housed two per ''shoe-box'' style cage and allowed to acclimate for 5 days before use. Animals had unrestricted access to PMI #5001 rodent chow (PMI feeds, St. Louis, MO) and water. Rats were kept in a humidity/climate-controlled facility with a 12-h light/dark cycle which is accredited by the American Association for Accreditation of Laboratory Animal Care (AAALAC). The study was conducted in accordance with the National Institutes of Health (NIH) guidelines for the care and use of laboratory animals. Rats were weighed upon dosing and on Days 5, 9, 15, and 22. The number of rats weighted per dose group per day diminished to an $n = 8$ by Day 22 post dosing. Rats were euthanatized by CO_2 asphyxiation.

Tissue collection and preparation. Blood was collected from the inferior vena cava using an 18½-gauge needle (Becton Dickinson) and 10-cc syringe (Becton Dickinson). Blood was placed into serum separator tubes, allowed to clot, and centrifuged for 15 min at room temperature. Serum aliquots were stored at −80°C until analysis of TSH and thyroid hormones. Blood and fat were also collect for analysis of PCB 126 (not reported). Livers were excised, and portions of the liver divided for analysis of cytochrome P450 (CYP) 1A1 activity, UDPGT activity, and Type I 5′-deiodinase activity (not reported). Hepatic protein content was measured using the method of Lowry *et al*. (1951). Another portion of the liver was frozen for later analysis of PCB 126.

Liver microsomes were prepared by taking 5 g of liver sample from each animal, homogenizing in 25 ml of 0.02 M Tris–HCl containing 0.15 M KCl (pH 7.4), and centrifuging at 10,000 × *g* for 30 min at 4°C. The pellet was then washed, resuspended in 0.25 M sucrose containing 10 mM EDTA and 1.15% KCl (pH 7.4), and stored at −80°C. Liver homogenates for Type I 5′-deiodinase activity were prepared by homogenizing 1 g of liver in 5 ml of a buffer containing 100 mM potassium phosphate, 1 mM ethylenediamine tetraacetate (EDTA), and 1 mM dithiothreitol (DTT) (pH 7.0) and stored at −80°C. Thyroids were carefully dissected free of fat and connective tissue, weighed, and placed in 10% formalin for histopathology to determine thyroid colloid volume/follicle epithelium volume ratios.

Analysis of PCB 126 in tissue. PCB 126 was extracted from liver by placing 0.3 g of tissue into a 20 ml vial containing 2 μl of an internal standard (4,4′-dibromobiphenyl) solution and 0.3 g of powered anhydrous sodium sulfate. Methanol (0.3 ml) and 5 ml of hexane were added, and the mixture homogenized (TISSUE TEAROR, Biospec Products, Inc.) for 1 min. The supernatant organic phase was transferred to a test tube and centrifuged at 3,500 rpm for 10 min, and 1.5 ml of the organic phase (hexane) was loaded onto a preconditioned (1 ml of hexane without vacuum) Bond Elut PCB cartridge (Varian, Inc.). One ml of hexane was used to elute the organic phase under light vacuum for 3 min. This step was repeated three additional times for an accumulated elution volume of 4 ml. The eluate was then concentrated to dryness under a mild stream of nitrogen and redissolved in 0.3 ml of hexane. Two μl of the sample was injected into a gas chromatograph (GC) equipped with a micro-electron capture detector (μECD) (Agilent 6890) and an Agilent autosampler 7683.

The oven condition was initially set to 100°C for 3 min, increased at a rate of 7°C/min to a temperature of 220°C, increased at a rate 3°C/min to a temperature of 260°C, and finally increased at a rate of 15°C/min to a temperature of 280°C. The run time was about 45 min for each sample. The inlet was 250°C

with a 20:1 split. A HP-5 capillary column (15 m × 0.53 mm × 1.5 μM) was used with an initial carrier flow rate of 2.2 ml/min. The μECD detector was heated to 300°C. Under the conditions described, the limit of quantification for PCB 126 in liver was 2.7 μg/kg. The average extraction efficiency was over 92% for liver.

Hepatic enzyme analysis. Ethoxyresorufin-O-deethylation (EROD) was measured as indicator of activity of CYP 1A1 on complete time-course data sets. The fluorimetric technique described by Lubet *et al*. (1985) was used to quantify EROD activity (nM/min/mg protein). This provided the rate of CYP 1A1–mediated deethylation of 7-ethoxyresorufin to resorufin. The Day 9 275-μg/kg liver samples for EROD analysis were not used because of experimental error.

Hepatic microsomal T_4-G (thyroxine glucuronide) formation rates catalyzed by uridine diphosphate glucuronyl transferases (UDPGTs) and glucuronic acid were assayed for the complete time-course data sets based on the method of Visser *et al*. (1993) as modified by Zhou *et al*. (2001). The calculated UDPGT activity was reported as pM T_4-G formed/mg protein/min. The limit of detection for UDPGT activity with T_4 as the substrate was 0.05 pM T_4-G/mg protein.

Serum hormone and TSH analyses. Serum fT_4 concentrations were measured on samples from Days 5 and 22 in all dose groups. Serum total T_4 (T_4), total T_3 (T_3), and reverse T_3 (rT_3) concentrations were collected on Days 5, 9, and 22 in all dose groups. Serum TSH was measured for all doses on days 5, 9, and 22.

Serum free thyroxine (fT_4) analysis by direct dialysis was carried out at first thaw of the serum aliquots to avoid altered serum binding due to repeated freeze-thaw cycles. Nondialysis fT_4 immunoassays often used in rat serum samples are designed for human serum samples, which have much higher concentrations of thyroxine binding globulin than animal sera (Refetoff *et al.*, 1970). Systematic underestimation of fT_4 has been documented to occur in animal and human sera (Nelson *et al.*, 2005; Rabin *et al.*, 2004; and Schachter *et al.*, 2004) when nondialysis fT_4 assays were employed. The fT_4 direct dialysis assay kit (Nichols Institute Diagnostics, Inc., San Clemente, CA) used in these studies involved the overnight dialysis of 200 μl of serum against 2.4 ml of buffer at 37°C prior to the sensitive radioimmunoassay of the dialysate for T_4. All samples were performed in the same assay. The immunoassay intra-assay variation of the high standard provided by the manufacturer was 5.9%, and the low standard was 10.0%.

Serum total T_4 and T_3 (not reported) were measured by radioimmunoassay (Chopra *et al.*, 1980; Eltom *et al.*, 1992) using the T_4-15 and T_3-38 antisera obtained from Endocrine Sciences (Calabasas, CA). Serum rT_3 concentrations (not reported) were measured in the same assay by radioimmunoassay as described by Ferguson and Peterson (1992) for dog serum, but modified for rat serum. All immunoassays included iodothyronine-free serum prepared by activated charcoal extraction of endogenous hormone as previously described (Eltom *et al.*, 1992). Radiolabeled T_4 (^{125}I-thyroxine, S.A. >1500 μCi/μg) was obtained from Amersham Biosciences, and radiolabelled T_3 (^{125}I-3,5,3′-triiodothyronine, S.A 1080–1320 μCi/μg) and rT_3 ([^{125}I] 3,3′,5′-triiodothyronine, S.A 1080–1320 μCi/μg) were obtained from Perkin Elmer (Boston, MA). The intra-assay coefficients of variation for the T_4, T_3, and rT_3 assays in this study were, respectively: 8.8%, 7.7%, and 29.7%. We would note that the rT_3 concentrations measured were quite low. The mean and standard deviation serum concentration of the chosen pool was 5.6 ± 1.7 ng/dl for an assay with a detection limit of 2 ng/dl.

Serum rat TSH concentrations were measured using a radioimmunoassay kit (ICN Diagnostics #07C-90102, Orangeburg, NY). The intra-assay coefficient of variation was 9.5%.

Thyroid histomorphometry. Thyroid glands were collected on Day 22 for all PCB 126 dose groups. Both thyroid glands from each rat were fixed in neutral buffered 10% formalin solution, embedded in paraffin, sectioned sagittally at 3 μm, and stained with hematoxylin and eosin. All sections were examined microscopically. To obtain a quantitative measure of the relative amount of colloid and follicular epithelial cell volume for each rat, a stereological procedure was performed. The volume fractions of follicular epithelial cells and of colloid were measured by a stereological technique using light microscopy at 200× and an eyepiece reticle (Russ, 1986). A grid with 121 equidistant points was placed over two midline sections of each thyroid gland, and volume fractions (V%) for colloid and follicular epithelium were calculated using the formula:

$$\%V = \frac{Pc}{Pt} \times 100 \quad \text{or} \quad \%V = \frac{Pe}{Pt} \times 100$$

respectively, where Pc is the number of points that intersected colloid, Pe is the number of points that intersected follicular epithelium, and Pt is the total number of points on the grid (Rongnoni *et al.*, 1989). All four measurements for each of the rats were averaged to obtain mean volume fractions. The colloid volume fraction (CV) to follicular volume fraction (FV) ratio for each rat was calculated using the formula:

$$\frac{CV}{FV} = \frac{\%\,V\ colloid}{\%\,V\ follicular\ epithelium}$$

Statistical analysis. Treatment-related effects at each time point were first evaluated with an analysis of variance followed by Dunnett's test ($p < 0.05$) for comparison of treatment means to control means. All analyses were performed using SAS V 8.2 (Cary, NC). Some of the data are presented as percent or fold changes from control values. Statistical analyses were carried as mentioned above, and an asterisk signifies a statistically significant difference from control ($p < 0.05$).

Berkley Madonna (Berkeley Madonna, Inc) software was used to perform linear interpolations and calculate dose-dependent time-integrated measures of mean hepatic PCB 126 concentrations, T_4-G production rates, and EROD activity, and serum TSH, and T_4 concentrations. Integrations were carried out for 22 days and then averaged on a daily basis. The integration method for stiff systems (Rosenbrock) was used.

RESULTS

Kinetics of PCB 126

Single oral bolus PCB 126 doses slowed mean body weight gain by Day 22 post dosing in the 75- and 275-μg/kg dose groups by 13 and 17%, respectively (Fig. 1a). Peak hepatic PCB 126 concentrations for the 7.5-, 75-, and 275-μg/kg dose groups were observed rapidly by Days 1, 3, and 1 post dosing, respectively. Hepatic clearance of PCB 126 was slow (Fig. 2a). The time-integrated liver exposure to PCB 126 or area-under-the-concentration-curve (AUCC) (μg/kg/day) was modestly curvilinear as a function of administered dose (Fig. 2b).

PCB 126 Dose- and Time-Dependent Perturbations in Hepatic Enzymes and the HPT Axis

Liver. Dose- and time-dependent increases in the hepatic rate of formation of T_4-G were observed for the two highest doses of PCB 126 (Fig. 3a). Peak induction of T_4-G formation rates occurred on Day 5 after dosing and was elevated 3.4- and 6.6-fold for the 75- and 275-μg/kg dose groups, respectively. The 7.5-μg/kg dose of PCB 126 did not induce significant increases in T_4-G production. The amount (pM) of T_4-G produced in the liver/mg of protein/day slowed at the 275-μg/kg dose and was not linearly related with the time-integrated (AUCC) hepatic concentration of PCB 126 (Fig. 3b).

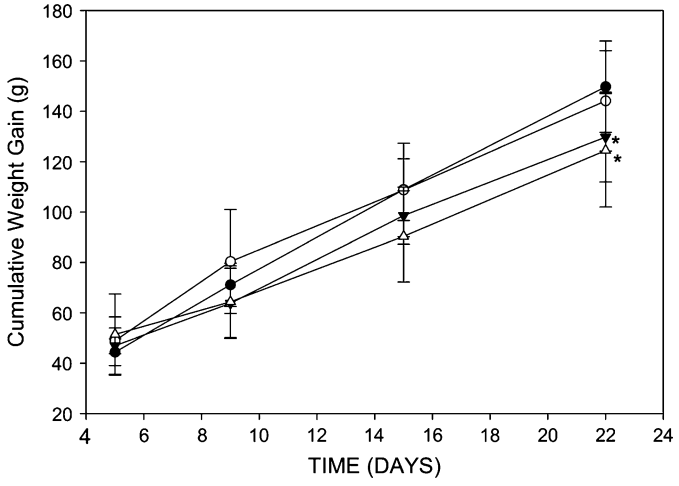

FIG. 1. Cumulative body weight gain (grams) for 22 days after administration of a single oral bolus dose of either control (●), 7.5 (○), 75.0 (▼), or 275 (△) μg/kg of PCB 126. Statistically significant deceases in weight gain are denoted with an asterisk (*).

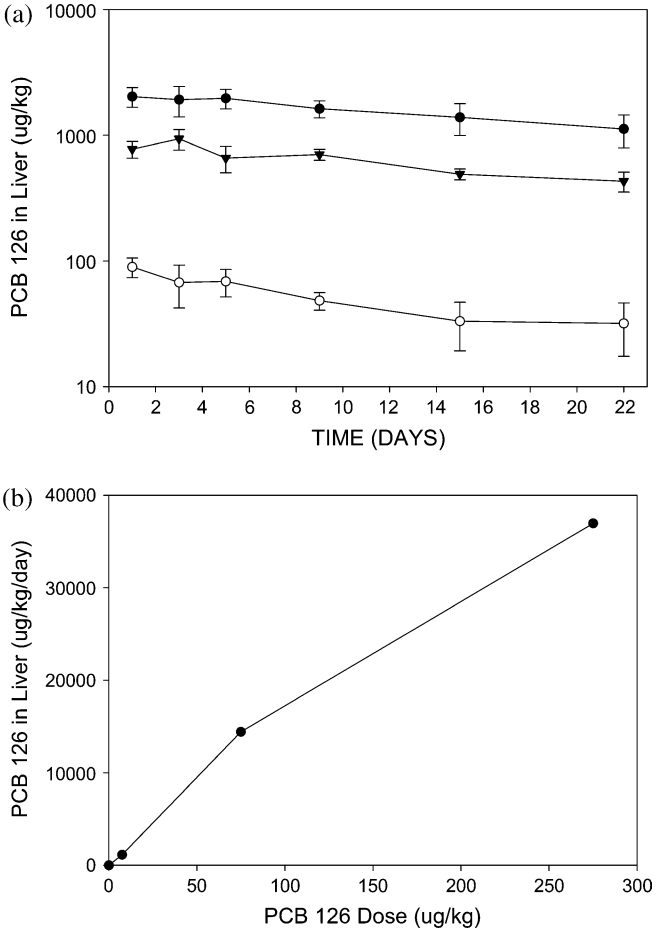

FIG. 2. (a) Measured concentrations of PCB 126 (μg/kg or ppb ± SD) in liver after administration of a single oral bolus dose of either 7.5, 75, or 275 μg/kg. (b) Administered dose of PCB 126 versus daily area-under-the-concentration curve for PCB 126 in liver for a 22-day period.

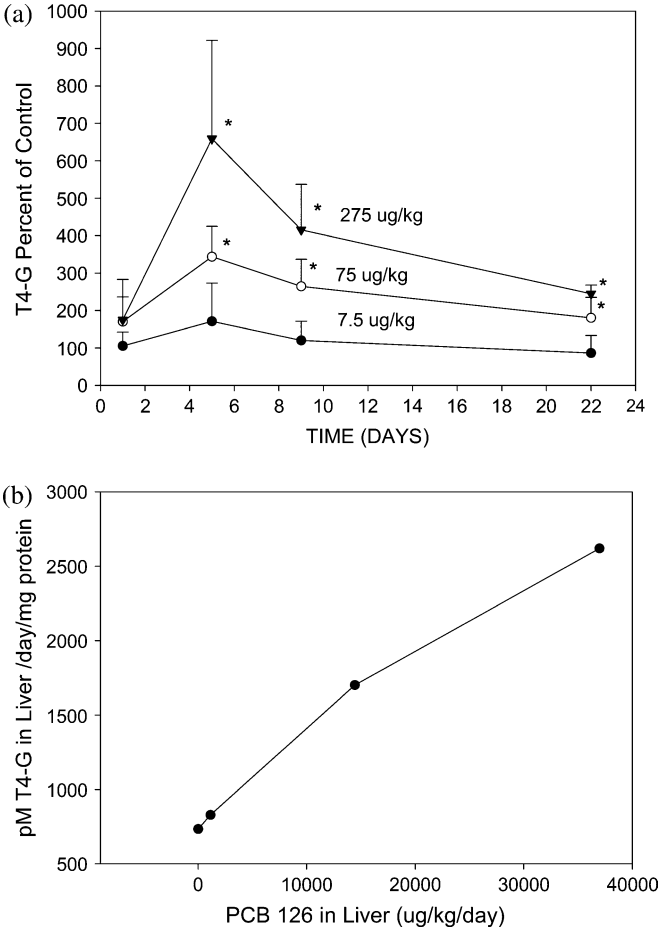

FIG. 3. (a) Time course for percent induction (±SD) of hepatic UDPGT activity compared to control (100%), measured as the rate of formation of thyroxine glucuronide (T_4-G, pM/min/mg protein). Statistically significant changes are denoted with an asterisk (*). (b) Daily area-under-the-concentration curve for PCB 126 in liver versus the daily production of thyroxine glucuronide (pM/ T_4-G/mg protein/day) for a 22-day period.

EROD activity was significantly increased for the study period in the two highest groups and only on Day 1 in the lowest dose group (Fig. 4a). Peak hepatic induction of CYP 1A1 activity (EROD) on Day 5 was similar for both the 75- and 275-μg/kg dose groups (about 30-fold), while the peak hepatic CYP 1A1 activity for the 7.5-μg/kg dose group was about 12-fold on Day 1. Interestingly, the daily EROD activity was linearly related with the time-integrated hepatic PCB 126 concentration (Fig. 4b) above ≈100 μM/mg protein/day or the lowest administered dose.

Serum. Serum T_4 and fT_4 concentrations were not altered by the lowest dose of PCB 126, while the two higher doses of PCB 126 caused a decline in serum T_4 and fT_4 concentrations (Figs. 5a and 5b) over the study period. Serum T_4 concentrations reached their nadir in the 75- and 275-μg/kg dose groups on Day 9. Serum fT_4 concentrations were only measured on Day 5 and 22. No dose-related changes were

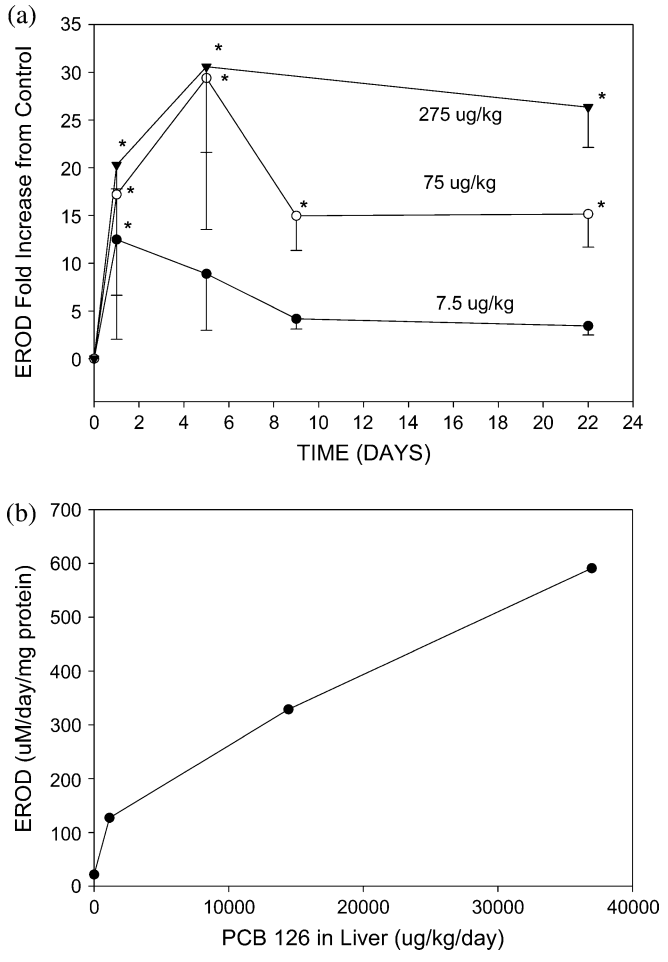

FIG. 4. (a) Time course for fold induction (±SD) of hepatic EROD activity (nM/min/mg protein) after administration of single oral bolus doses of PCB 126. Statistically significant changes are denoted with an asterisk (*). (b) Daily area-under-the-concentration curve for PCB 126 in liver versus the amount of daily EROD activity (μM/mg protein/day) for a 22-day period.

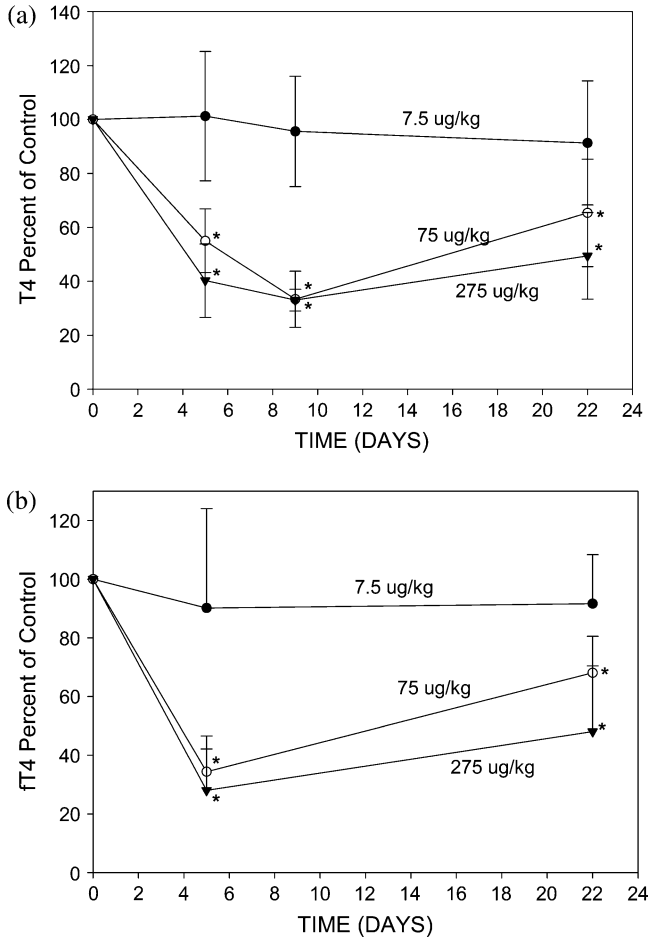

FIG. 5. Time course for (a) serum T_4 (ug/dl) and (b) fT_4 (ng/dl) expressed as a percent of control (100%) ± SD. Statistically significant changes are denoted with an asterisk (*).

observed in serum T_3 or rT_3 concentrations, except for transient decreases in T_3 on Day 22 and rT_3 on Day 5 (data not shown).

The two highest PCB 126 doses caused increases in serum TSH concentrations (Fig. 6) over the study period. Surprisingly, the mean serum TSH concentrations for the 75- and 275-μg/kg dose groups were similar. The reason for this is unknown. Serum TSH concentrations were not significantly elevated in the 7.5-μg/kg dose group.

Thyroid. Microscopically, all thyroid glands appeared normal, i.e., there was no evidence of gross thyroid hyperplasia. Follicular size and staining intensity of colloid varied considerably within individual thyroid glands. Qualitatively, a modest increase in the size and height of the follicular epithelium and decrease in size of follicular lumens was noted in rats receiving the 75-and 275-μg/kg dose on Day 22 post dosing. Quantitatively, the ratio of colloid volume fraction/follicular epithelial volume fraction was significantly lower (Table 1) in only the 275-μg/kg dose group on Day 22. A lower CV/FV is a morphologic indicator consistent with the bioactivity of increased serum TSH concentrations.

DISCUSSION

The objective of these experiments was to gain insights into the time- and dose-dependent nature of PCB 126 induction of hepatic UDPGT which results in increased phase II metabolism and systemic clearance of thyroxine (T_4). As a consequence of increased metabolism of T_4 to thyroxine glucuronide (T_4-G), the hypothalamus/pituitary responds to lowered serum levels of T_4 by releasing increased amounts of TSH (negative feedback) into the blood supply. TSH then binds to receptors on the thyroid gland and upregulates the production of thyroid hormones. In our study we found that hepatic metabolism of T_4 was not induced 1 day post dosing, but by 5 days post dosing the hepatic metabolism was induced in the 75- and 275-μg/dose groups. Serum T_4 concentrations were also less than controls

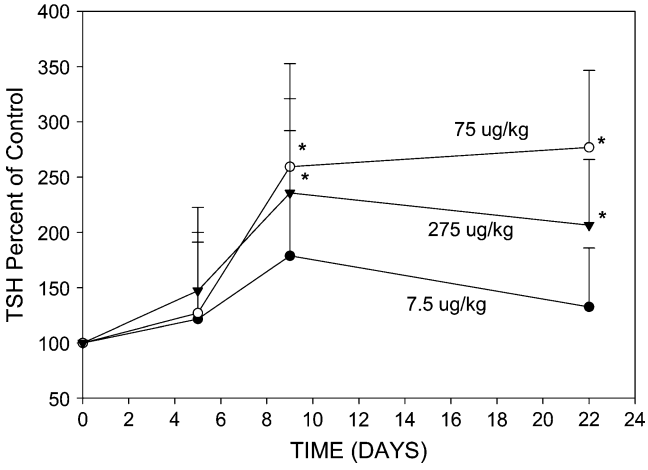

FIG. 6. Time course for serum TSH (ng/ml) ± SD expressed as percent of control (100%). Statistically significant changes are denoted with an asterisk (*).

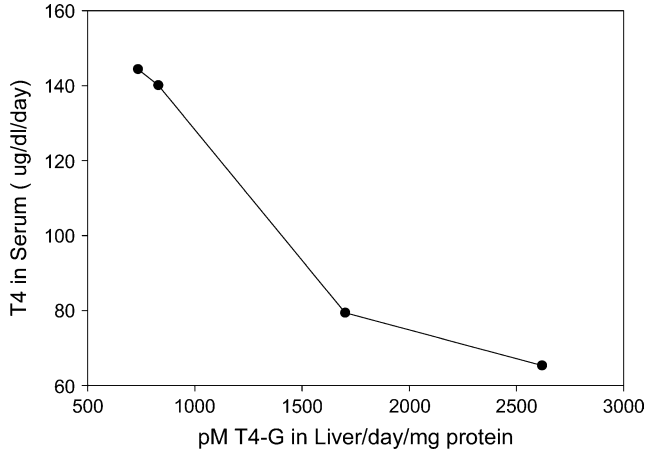

FIG. 7. Amount of thyroxine glucuronide produced in the liver per day/mg protein versus the daily area-under-the-concentration-curve for serum T_4 for a 22-day period.

by Day 5 post dosing in these dose groups. Serum TSH was not elevated by Day 5, suggesting that sustained low serum T_4 concentrations were not yet sufficient (negative feedback loop) to upregulate production of TSH. However by Day 9 post dosing, serum TSH concentrations were elevated in these dose groups. The partial recovery of serum T_4 and fT_4 by 22 days post dosing is because hepatic UDPGT activity was slowly returning to a control level, and serum TSH continued to stimulate the thyroid gland. Morphometric analysis of the thyroid gland on Day 22 indicated that the gland was still stimulated by TSH by the 275-μg/kg dose. In the low-dose PCB 126 rats, a consistent negative response was found for hepatic UDPGT activity and serum TSH and thyroid hormones; only hepatic EROD activity was increased.

Using pharmacokinetic tools to analyze the data, we examined the relationships between internal dose of PCB 126 (liver) and perturbations in the HPT axis. A clear inverse relationship was observed between the daily amount of T_4 metabolized to T_4-G and the AUCC values for T_4 in serum (Fig. 7). This provides strong kinetic support for induction of UDPGTs as the primary mechanism of action for PCB 126 on the HPT axis. At the 275-μg/kg dose of PCB 126, compensatory mechanisms may have maintained the time-integrated serum T_4 concentrations despite a continued rise in induction of hepatic UDPGT activity. This resulted in less than expected decrease in serum AUCC T_4 values (Fig. 7) or nonlinear kinetic behavior. When evaluating the inverse relationship between the time-integrated concentrations (AUCC) of TSH and serum T_4, the AUCC TSH values for the 75-μg/kg PCB 126 dose were apparently similar or greater than the 275-μg/kg dose (Fig. 8). This suggests that that sustained TSH production may have been compromised in the 275-μg/kg dose group. Fig. 8 demonstrates the nonlinear relationship between serum T_4 and TSH systemic availability, suggesting possible saturation of regulatory elements in the HPT axis. Taken together, these observations demonstrate that the HPT axis is a highly nonlinear system when disturbed by PCB 126 and will require the use of PBPK models to describe this endocrine system.

TABLE 1
Thyroid Gland: Colloid Volume Fraction/Follicular Epithelium Volume Fraction (±SD)

Dose (μg/kg)	Colloid volume/follicular epithelium volume fraction (±SD)
	Day 22
275	0.51 (0.15)*
75	0.55 (0.20)
7.5	0.84 (0.27)
Control	0.89 (0.43)

*Statistically significant change compared to control.

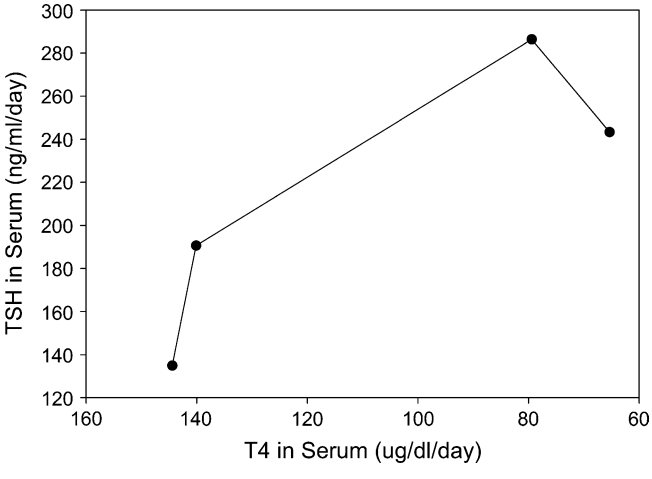

FIG. 8. The daily area-under-the-concentration-curve for serum T_4 versus the daily area-under-the-concentration-curve for TSH in serum for a 22-day period.

Other mechanisms that may disturb the HPT axis include hydroxyl metabolites of PCB 126 (Lans *et al*., 1993), which may displace thyroid hormones bound to serum proteins, although PCB 126 is cleared from the body very slowly by fecal excretion and metabolism, suggesting the role of metabolism may be minimal. The inclusion of induction of hepatic EROD (CYP1A1) activity is needed for the HPT axis to help understand how PCB 126 apportions itself between the AhR and CYP1A2 binding sites, and CYP1A1 induction may play a role in metabolism of PCB 126. The importance of CYP1A1 will become more apparent when a PBPK model for PCB 126 is developed.

In this study, T_4-G formation rates were increased to a maximum of 3.4- and 6.6-fold 5 days after dosing in the 75- and 275-μg/kg PCB 126 dose groups, respectively. Craft *et al*. (2002) reported approximately 3.5- and 7.4-fold inductions of T_4-G in rats 1 day after daily dosing for 4 days with 10 and 40 μg/kg of PCB 126. Kohn *et al*. (1996) developed a PBPK model for dioxin and its disturbances of the HPT axis and surmised that the excretion of T_4-G from the body was the primary mode of action. There was very little kinetic data in this study to validate these conclusions.

PCB 126 concentrations were much greater in liver than in fat (data not shown), indicating that binding of PCB 126 to hepatic-derived CYP 1A2 is substantial (Chen *et al.*, 2003). These findings are consistent with other studies that have compared PCB 126 concentrations in liver and fat after administration of PCB 126 (Angelique *et al.*, 1994; Chen *et al.*, 2001; Lyche *et al.*, 2004). Both CYP 1A1 and CYP 1A2 catalyze the metabolism of many xenobiotics and have broad ligand specificities. There is a much greater amount of CYP 1A2 in rat liver than CYP 1A1. The high-affinity binding of PCB 126 to CYP 1A2 results in competitive inhibition of CYP 1A2 (methoxyresorufin, MROD) activity, with an inhibition constant (Ki) equal to 0.026 μM (Chen *et al.*, 2003). On the other hand, CYP 1A1 (EROD) activity was highly induced by PCB 126. Hepatic induction of EROD (CYP 1A1) by PCB 126 has been reported in several *in vitro* and *in vivo* studies, with some studies focused on the HPT axis (Craft *et al.*, 2002; Desaulniers *et al.*, 1999; Martin, 2002). CYP 1A1 has been reported to be induced with PCB 126 as great as 95-fold in rats (Toyoshiba *et al.*, 2004) and up to 1000-fold induction has been reported in hepatic cells (CYP 1A1 mRNA) (Broccardo *et al.*, 2004).

Eltom *et al*. (1992) showed the TCDD affected 5′-deiodianse activity (possibly directly) in thyroidectomized rats despite T_3 replacement therapy. Usually the serum T_3 and rT_3 concentrations reflect the status of Type I 5′-deiodinase activity. T_3 serum concentrations in this acute dosing study did not change appreciably, but chronic administration of PCB 126 causes an increase in serum T_3 and TSH concentrations and a decrease in T_4 concentrations (NTP, 2005). We speculate that, in the NTP study with PCB 126, adaptive responses occurred to maintain T_3 concentrations, such as a decrease in metabolism of T_3 or increased production of T_3 by the thyroid (Schuur *et al.*, 1997).

Our findings differ in some respects from previous acute dosing studies with PCB 126 in rats. TSH serum levels were increased in this study, while Desaulniers *et al*. (1999) and Martin (2002) reported no changes in serum TSH concentrations. Desaulniers *et al*. (1999) also reported reductions in total T_3 serum concentrations, which was not the case in this study. On the other hand, in the present study a morphometric analysis of the thyroid gland revealed a typical pattern of decreased colloid, indicating TSH stimulation of the thyroid gland. Desaulniers *et al.* (1999) also analyzed the histology of the thyroid glands of PCB 126-treated animals and found that the colloid was less dense than in control animals, which is consistent with depletion by TSH stimulation.

To our knowledge, this is one of the first studies to apply the technique of fT_4 measurements by equilibrium dialysis to studies of toxin effects on thyroid hormone metabolism. Several studies of PCBs and the thyroid axis in nonprimate species showed declines in serum fT_4 concentrations using nondialysis methodology. Nondialysis procedures are generally not accurate in nonprimate species because of the lower amount of the high-affinity binding protein, thyroid binding globulin (TBG), in these species. This results in an underestimation of the fT_4 concentrations in serum by analog procedures (Nelson, 2005; Schachter *et al.*, 2004).

In conclusion, our pharmacokinetic study suggests that the primary mode of action of PCB 126 on the HPT axis in the adult male Sprague Dawley rat is increased phase II metabolism of thyroxine, presumably mediated by AhR. Recent studies with nuclear receptors indicate that nuclear receptors exhibit cross talk and coordinated cellular activities, suggesting that other receptors play important roles in thyroid hormone homeostasis (Bock and Köhle, 2004), particularly as it relates to chemical/drug-specific disturbances in the HPT axis. Our pharmacokinetic analysis suggests that the dose-response characteristics of PCB 126–induced perturbations in the HPT axis are complex and nonlinear. The design of experimental studies, such as this study, to examine both the temporal- and dose-dependent changes in the HPT axis is important for the development of dose-response curves for thyroid-active chemicals. The development of a PBPK model for the HPT axis will aid in understanding complex nonlinear dose-response data for thyroid active chemicals.

ACKNOWLEDGMENTS

Primary support for this research was kindly provided by ATSDR grant U61/ATU472105-(02, 03, and 04). Additional support was provided by U.S. EPA, ORD/NHEERL and the University of Georgia, College of Agricultural and Environmental Sciences. Special thanks to Deirdre Mahle, John Swint, Wilson Everett, Andy Smith, and Reiko Perleberg for helping with the animal studies. This manuscript has been reviewed by the National Health and Environmental Effects Research Laboratory, U.S. Environmental Protection Agency, and approved for publication. Mention of trade names or commercial products does not constitute endorsement or recommendation for use.

REFERENCES

Auyeung, D. J., Kessler, F. K., and Ritter, J. K. (2003). Mechanism of rat UDP-glucuronosyltransferase 1A6 induction by oltipraz: Evidence for a contribution of the Aryl hydrocarbon receptor pathway. *Mol. Pharmacol.* **63,** 119–127.

Angelique, P., Van Birgelen, J. M., Van Der Kolk, J., Fase, K. M., Bol, I., Poiger, H., Brouwer, A., Brower, A., and Van Den Berg, M. (1994). Toxic potency of 3,3′,4,4′,5-pentachlorobiphenyl relative to and in combination with 2,3,7,8-tetrachlorodibenzo-*p*-dioxin in a subchronic feeding study in the rat. *Toxicol. Sci.* **127,** 209–221.

ATSDR (Agency for Toxic Substances and Disease Registry) (2000). Toxicological profile for polychlorinated biphenyls (PCBs). http://www.atsdr.cdc.gov/toxprofiles/tp17-p.pdf.

Beetstra, J. B., van Engelen, J. G., Karels, P., van der Hoek, H. J., de Jong, M., Docter, R., Krenning, E. P., Hennemann, G., Brouwer, A., and Visser, T. J. (1991). Thyroxine and 3,3′,5-triiodothyronine are glucuronidated in rat liver by different uridine diphosphate-glucuronyltransferases. *Endocrinology* **128,** 741–746.

Bock, K. W., and Köhle, C. (2005). Coordinate regulation of drug metabolism xenobiotic nuclear receptors: UGTs acting together with CYPs and glucuronide transporters. *Drug Met. Disp.* **36,** 595–615.

Broccardo, C. J., Billings, R. E., Chubb, L. S., Andersen, M. E., and Hannelman, W. H. (2004). Single cell analysis of switch-like induction of CYP 1A1 in liver cells lines. *Toxicol. Sci.* **78,** 287–294.

Brouwer, A., Morse, D. C., Lans, M. C., Schuur, A. G., Murk, A. J., Klasson-Wehler, E., Bergman, A., and Visser, T. J. (1998). Interactions of persistent environmental organohalogens with the thyroid hormone system: Mechanisms and possible consequences for animal and human health. *Toxicol. Ind. Health* **14,** 59–84.

Chauhan, K. R., Kodavanti, P. R., and McKinney, J. D. (2000). Assessing the role of ortho-substitution on polychlorinated biphenyl binding to transthyretin, a thyroxine transport protein. *Toxicol. Appl. Pharmacol.* **162,** 10–21.

Cheek, A. O., Kow, K., Chen, J., and McLachlan, J. A. (1999). Potential mechanisms of thyroid disruption in humans: Interaction of organochlorine compounds with thyroid receptor, transthyretin, and thyroid-binding globulin. *Environ. Health Perspect.* **107:** 273–278.

Chen, J. J., Chen, G. S., and Bunce, N. J. (2003). Inhibition of CYP 1A2-dependent MROD activity in rat liver microsomes: An explanation of the hepatic sequestration of a limited subset of halogenated aromatoc hydrocarbons. Wiley InterScience (www.interscience.wiley.com), Wiley Periodicals, Inc.

Chen, C.-Y., Hamm, J. T., Hass, J. R., and Birnbaum, L. S. (2001). Disposition of olychlorinated dibenzo-*p*-dioxins, dibenzofurans, and non-ortho polychlorinated biphenyls in pregnant long evans rats and the transfer to offspring. *Toxicol. Appl. Pharmacol.* **173,** 65–88.

Chopra, I. J., Van Herle, A. J., Teco, G. N., and Nguyen, A. H. (1980). Serum free thyroxine in thyroidal and nonthyroidal illnesses: A comparison of measurements by radioimmunoassay, equilibrium dialysis, and free thyroxine index. *J. Clin. Endocrinol. Metab.* **51,** 135–143.

Craft, E. S., DeVito, M. J., and Crofton, K. M. (2002). Comparative responsiveness of hypothyroxinemia and hepatic enzyme induction in Long-Evans rats versus C57BL/6J mice exposed to TCDD-like and phenobarbital-like polychlorinated biphenyl congeners. *Toxicol. Sci.* **68,** 372–380.

Desaulniers, D., Leingartner, K., Wade, M., Fintelman, E., Yagminas, A., and Foster, W. G. (1999). Effects of acute exposure to PCBs 126 and 153 on anterior pituitary and thyroid hormones and FSH isoforms in adult Sprague Dawley male rats. *Toxicol. Sci.* **47,** 158–169.

DeVito, M. J., Maier, W. E., Diliberto, J. J., and Birnbaum, L. S. (1993). Comparative ability of various PCBs, PCDFs, and TCDD to induce cytochrome P450 1A1 and 1A2 activity following 4 weeks of treatment. *Toxicol. Appl. Pharmacol.* **20,** 125–130.

Eltom, S. E., Babish, J. G., and Ferguson, D. C. (1992). The interaction of L-triiodothyronine and 2,3,7,8-tetrachlorodibenzo-*p*-dioxin on Ah-receptor-mediated hepatic Phase I and Phase II enzymes and iodothyronine 5′-deiodinase in thyroidectomized rats. *Toxicol. Lett.* **61,** 125–139.

Ferguson, D. C., and Peterson, M. E. (1992). Serum free and total iodothyronine concentrations in dogs with hyperadrenocorticism. *Am. J. Vet. Res.* **53,** 1636–1640.

Hood, A., and Klaassen, C. D. (2000). Effects of microsomal enzyme inducers on outer-ring deiodinase activity toward thyroid hormones in various rat tissues. *Toxicol. Appl. Pharmacol.* **163,** 240–248.

Khan, M. A., and Hansen, L. G. (2003). *ortho*-Substituted polychlorinated biphenyl (PCB) congeners (95 or 101) decrease pituitary response to thyrotropin releasing hormone. *Toxicol. Lett.* **144,** 173–182.

Kohn, M. C., Sewall, C. H., Lucier, G. W., and Portier, C. J. (1996). A mechanistic model of effects of dioxin on thyroid hormones in the rat. *Toxicol. Appl. Pharmacol.* **136,** 29–48.

Kretschmer,C., and Baldwin, W. S. (2005). CAR and PXR: Xenosensors of endocrine disruptors? *Chem. Bio. Inter.* **155,** 111–128.

Lans, M. C., Klasson-Wehler, E., Willemsen, M., Meussen, E., Safe, S., and Brouwer, A. (1993). Structure-dependent, competitive interaction of hydroxy-polychlorobiphenyls, -dibenzo-*p*-dioxins and -dibenzofurans with human transthyretin. *Chem. Biol. Interact.* **88,** 7–21.

Li, M.-H., and Hansen, L. G. (1997). Consideration of enzyme and endocrine interactions in the risk assessment of PCBs. *Rev. Toxicol.* **1,** 71–156.

Lowry, O. H., Rosebrough, N. J., Farr, A. L., and Randall, R. J. (1951). Protein measurement with the Folin phenol reagent. *J. Biol. Chem.* **193,** 265–275.

Lubet, R. A., Mayer, R. T., Cameron, J. W., Nims, R. W., Burke, M. D., Wolff, T., and Guengerich, H. P. (1985). Dealkylation of pentoxyresorufin: A rapid and sensitive assay for measuring induction of cytochrome(s) P-450 by phenobarbital and other xenobiotics in the rat. *Arch. Biochem. Biophys.* **238,** 43–48.

Lyche, J. L., Skaare, J. U., Larsen, H. J. S., and Ropstad, E. (2004). Levels of PCB 126 and PCB 153 in plasma and tissues in goats exposed during gestation and lactation. *Chemosphere* **55,** 621–629.

Martin, L. A. (2002). Differential effects of polychlorinated biphenyl (PCB) mixtures and congeners on the disposition of thyroxine(T4). Ph.D. Dissertation, Rutgers the State University of New Jersey, New Brunswick, NJ.

Nelson, J. C., Wang, R., Asher, D. T., and Wilcox, R. B. (2005). Underestimates and overestimates of total thyroxine concentrations caused by unwanted thyroxine-binding protein effects. *Thyroid* **15,** 12–15.

NTP. (National Testing Program) (2005). TR-520 Toxicology and Carcinogenesis Studies of 3,3′,4,4′,5-Pentachlorobiphenyl (PCB 126) (CAS No. 57465–28–8) in Female Harlan Sprague-Dawley Rats (Gavage Studies) (draft). http://ntp.niehs.nih.gov/index.cfm?objectid=070B63EC-0CA5-F40D-5A3246E781C31164.

Rabin, C. W., Hopper, A. O., Job, L., Peverini, R. L., Clark, S. J., Deming, D. D., Nelson, J. C., and Vyhmeister, N. R. (2004). Incidence of low free T4 values in premature infants as determined by direct equilibrium dialysis. *J. Perinatol.* **24,** 640–644.

Refetoff, S., Robin, N. I., and Fang, V. S. (1970). Parameters of thyroid function in serum of 16 selected vertebrate species: A study of PBI, serum T4, free T4, and the pattern of T4 and T3 binding to serum proteins. *Endocrinology* **86,** 793–805.

Rongnoni, J. B., Penel, C., Bastiani, P., Roccabianca, M., and Lemarchand-Beraud, Th. (1989). Down regulation of hypertrophied follicular cell volume in thyroid hyperplastic gland. *Histol. Histopathol.* **4,** 193–200.

Russ, J. C., Hare, T. M., Christensen, R. P., Hare, K. T., and Russ, J. C. (1986). SEM low magnification stereoscopic technique for mapping surface contours: Application to measurement of volume differences in human teeth due to polishing. *J. Microsc.* **144,** 329–338.

Schachter, S., Nelson, R. W., Scott-Moncrieff, C., Ferguson, D. C., Feldman, E. C., Montgomery, T., and Neal, L. (2004). Comparison of serum free thyroxine concentration determined by standard equilibrium dialysis, modified equilibrium dialysis, and five radioimmunoassays in dogs. *J. Vet. Int. Med.* **18,** 259–264.

Schuetz, E. G., Brimer, C., and Schuetz, J. D. (1998). Environmental xenobiotics and the antihormones cyproterone acetate and spironolactone use the nuclear hormone pregnenolone X receptor to activate the CYP3A23 hormone response element. *Mol. Pharmacol.* **54,** 1113–1117.

Schuur, A. G., Boekhorst, F. M., Brouwer, A., and Visser, T. J. (1997). Extrathyroidal effects of 2,3,7,8-tetrachlorodibenzo-*p*-dioxin on thyroid hormone turnover in male Sprague-Dawley rats. *Endocrinology* **138,** 3727–3734.

Toyoshiba, H., Walter, N. J., Bailer, A. J., and Portier, C. J. (2004). Evaluation of toxic equivalency factors for induction of cytochromes P450 CYP 1A1 and CYP 1A2 enzyme activity by dioxin-like compounds. *Toxicol. Appl. Pharmacol.* **194,** 156–168.

Van Birgelen, A. P., Van der Kolk, J., Fase, K. M., Bol, I., Poiger, H., Brouwer, A., Van den Berg, M. (1994a). Toxic potency of 3,3′,4,4′,5-pentachlorobiphenyl relative to and in combination with 2,3,7,8-tetrachlorodibenzo-*p*-dioxin in a subchronic feeding study in the rat. *Toxicol. Appl. Pharmacol.* **127,** 209–221.

Van Birgelen, A. P., Van der Kolk, J., Fase, K. M., Bol, I., Poiger, H., Van den Berg, M., and Brouwer, A. (1994b). Toxic potency of 2,3,3′, 4,4′,5-hexachlorobiphenyl relative to and in combination with 2,3,7,8-tetrachlorodibenzo-*p*-dioxin in a subchronic feeding study in the rat. *Toxicol. Appl. Pharmacol.* **126,** 202–213.

Visser, T. J., Kaptein, E., van Toor, H., van Raaij, J. A. G. M., van den Berg, K. J., Joe, C., vanEngelen, J. G. M., and Brouwer, A. (1993). Glucuronidation of thyroid hormone in rat liver: Effects of *in vivo* assay conditions. *Endocrinology* **135,** 2177–2186.

Yoshimura, H., Yoshihara, S., Koga, N., Nagata, K., Wada, I., Kuroki, J., and Hokama, Y. (1985). Inductive effect on hepatic enzymes and toxicity of congeners of PCBs and PCDFs. *Environ. Health Perspect.* **59,** 113–119.

Zhou, T., Ross, D. G., De Vito, M. J., and Crofton, K. M. (2001). Effects of short-term *in vivo* exposure to polybrominated diphenyl ethers on thyroid hormones and hepatic enzyme activities in weanling rats. *Toxicol. Sci.* **61,** 76–82.